Astron. Astrophys. 361, 444–450 (2000)

ASTRONOMY AND ASTROPHYSICS

Multiwavelength observations of the field HS47.5/22 in Ursa Major⋆

II. AGN statistics

K. Molthagen

[1] Max–Planck–Institut für Extraterrestrische Physik, 85740 Garching, Germany
[2] Hamburger Sternwarte, Gojenbergsweg 112, 21029 Hamburg, Germany

Received 3 June 1999 / Accepted 12 July 2000

Abstract. An analysis is given of the AGN found in the medium deep X–ray survey in the HQS field HS 47.5/22 . The $\log N(>S) - \log S$ curve is in good agreement with values in the literature above $\mathrm{f_x} \simeq 3.4 \cdot 10^{-14}\ \mathrm{ergs\,cm^{-2}\,s^{-1}}$. Redshifts are now determined for 71 AGN detected in the X–ray survey. Complete optically and X–ray selected samples were derived. In the optical range, we find a completeness limit of $\mathrm{m_b} = 18\overset{\mathrm{m}}{.}3 - 18\overset{\mathrm{m}}{.}5$, resulting in a complete optical sample of not more than 18 AGN. X–ray completeness is primarily determined by the identification status. Below $2 \cdot 10^{-13}\ \mathrm{ergs\,cm^{-2}\,s^{-1}}$, more than 10% of the X–ray sources remain unidentified giving a complete sample of 26 AGN. Both the optical number-magnitude relation and the X–ray luminosity functions are in agreement with previous determinations. Thus we found no supporting evidence that this area in the sky shows a non-random AGN distribution. A few individual objects are described in detail, among them RX J1001.5+4659 - a possibly extended source connected to a small group of galaxies, and RX J0957.1+4815 - an X–ray selected QSO with deep absorption lines, perhaps a BAL.

Key words: galaxies: quasars: general – galaxies: quasars: individual: RX J0957.1+4815 – galaxies: quasars: individual: RX J0953.9+4617 – X-rays: galaxies

1. Introduction

The Hamburg Quasar Survey (HQS, Hagen et al. 1995) is an objective prism plate–based search in the northern hemisphere. One of its fields, HS 47.5/22, was chosen for multiwavelength follow–up observations. Radio, optical and especially X–ray data were presented by Molthagen et al. (1997, henceforth Paper I). The latter covered roughly $11\,\mathrm{deg^2}$ with the ROSAT PSPC. The results were presented in a source table with more than 500 entries which will be called XHS 47.5/22.

One of the reasons for choosing just this area for a follow–up study of HQS results was a conspicuous apparent non–random quasar distribution (see e.g. Fig. 1 of Paper I). Thus a closer look on the AGN is presented here.

After briefly describing the data in Sect. 2 the completeness of the X–ray catalogue will be determined and complete X–ray and optically selected AGN samples (mainly via $\log(f_\mathrm{x}/f_\mathrm{b})$) will be established in Sects. 3 and 4. Corresponding luminosity functions are computed in Sect. 5. A few individual objects will be discussed in some detail in Sect. 6.

2. The data

A detailed description of the analysis, a list of the pointings, the source catalogue with identifications, and the follow–up spectroscopy can be found in Paper I. In brief, the observations of XHS 47.5/22 consist of 48 overlapping pointings with the ROSAT PSPC (Pfeffermann et al. 1986; Trümper 1983). Various source detection runs were performed on the individual pointings as well as on the merged data. As pointed out in Paper I, not all sources which were found when working on individual OBIs or pointings could be seen in the merged data. This is entirely due to the fact that quite a number of sources exhibits variability over the 2.5 years of data–taking, coming out below the detection threshhold of the merged data set.

Obvious stellar counterparts (about 80) were deleted from the catalogue. For identifications of an X–ray source with a stellar–looking optical object without a z determination a $\log(f_\mathrm{x}/f_\mathrm{b})$ test was performed. In general, entries with $\log(f_\mathrm{x}/f_\mathrm{b}) > -1$ are regarded as extragalactic (Molthagen 1996). In this way a total extragalactic content of about 350 sources was determined.

The optical data of the AGN were taken from Véron-Cetty & Véron (1996), from the HQS identifications (Engels et al. 1998), or were observed during a 5 nights period in March 1994 with the 3.5 m telescope at Calar Alto/Spain (Paper I). The HQS found 27 AGN (three previously known) in XHS 47.5/22 (Engels et al. 1998), 22 of which were detected in our X–ray survey. A total of 41 new AGN was verified in Paper I. Two more sources

Send offprint requests to: H.J. Wendker, Hamburger Sternwarte (hjwendker@hs.uni-hamburg.de)

⋆ Partly based on observations from the German-Spanish Astronomical Center, Calar Alto, operated by the Max-Planck-Institut für Astronomie, Heidelberg, jointly with the Spanish National Commission for Astronomy

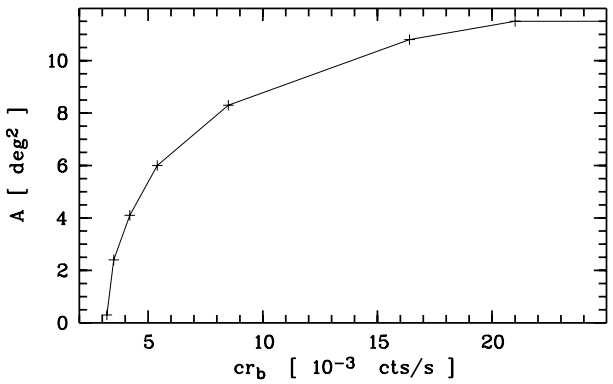

Fig. 1. Accessible area A as a function of limiting broad band count rate $cr_{\rm b}$.

(RX J0953.9+4617 and RX J0952.5+4603, see Sect. 6.1) have been observed since Paper I, and the former turned out to be an AGN. Two further X–ray selected quasars (RX J0947.0+4721 and MS 0944.1+4629) were added from the literature. The census of AGN with a z determination in XHS 47.5/22 stands now at 71.

3. log N − log S of the X–ray catalogue

The integral $\log N - \log S$ curve is computed for the above–described sample using

$$N(>S) = \sum_{>S} \frac{1}{A_i} \quad \text{, with error} \quad \sigma_N = \left[\sum_{>S} \frac{1}{A_i^2}\right]^{1/2}.$$

$A_{\rm i}$ is the area which was searched to find object i. A power law spectrum with $\alpha_{\rm E} = 1$ is assumed for all sources but they are individually corrected for galactic $\rm N_H$. Bias corrections as discussed by Hasinger et al. (1993, H93) and Vikhlinin et al. (1995a) are not applied because the differences between the source lists from the individual pointings and the merged data produce larger changes.

The accessible area for each source has to be carefully determined. Limiting count rates as a function of net exposure time (and consequently of area) have been determined for the broad and hard band of the merged data in Paper I (Table 1). Interpolations between tabulated values are used to determine the area A in which a source of count rate cr could have been detected. Table 4 in Paper I contains limiting count rates for each pointing at $\phi_{\rm oa} = 0'$ and $\phi_{\rm oa} = 40'$. Fig. 1 shows A as a function of the limiting count rate. Only sources detectable at $\phi_{\rm oa} = 40'$ in the shortest 'edge pointing' will be visible over the entire $11.5\,\deg^2$.

Using the same detection threshold of $\rm ML_{exi} = 10$ as H93 and Vikhlinin et al. (1995b, VFJM2) to ensure comparability a total of 351 sources remained in the merged catalogue. The resulting $\log N - \log S$ dependence is shown in Fig. 2. The curve is fairly well represented by a single power law. At fluxes above $3.4 \cdot 10^{-14}\ \rm ergs\,cm^{-2}\,s^{-1}$, the slope and normalization are $\gamma_{\rm m} = -1.71 \pm 0.14$ and $\log \rm K_m = -21.2 \pm 1.8$. The fit results are plotted as a dotted line in Fig. 2. Best fits from

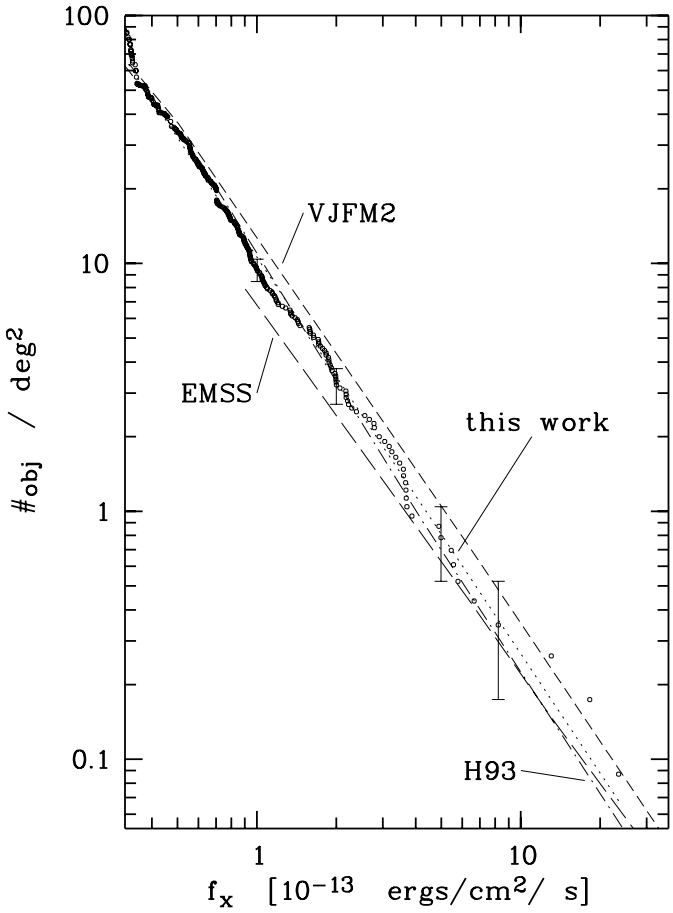

Fig. 2. $\log N - \log S$ curve derived from the merged data (dots) and our best fit. For clarity, only a few representative error bars have been included in the plot. Fluxes are in the total ROSAT band (0.1 – 2.4 keV); a conversion factor of 2.29 has been used to transform the results of H93 and VJFM2 to the total ROSAT band, and a factor 1.29 to convert the EMSS $\log N - \log S$ relation (Gioia et al. 1990).

the literature, H93, VFJM2 and the EMSS (Gioia et al. 1990) are also displayed. The agreement with these previous results is satisfactory. At a second glance such a close agreement is a little bit surprising because quite a number of stars were omitted in our work but not in the lists of H93 and VFJM2, and one might expect their number counts to be higher. The reason could simply be that H93 and VFJM2 only use hard band detections which do not favour stellar counterparts.

The apparent distortion above $\rm f_x = 10^{-12}\,ergs\,cm^{-2}\,s^{-1}$ is caused by three sources and thus explained by low statistics. A steepening just below $\rm f_x \simeq 3.4 \cdot 10^{-14}\ ergs\,cm^{-2}\,s^{-1}$ is most probably not real. Sources found here are likely to be affected by selection biases which lead to overestimated fluxes. These same problems also prohibit any attempts to determine from our data the resolved fraction of the X–ray background and the break fluxes found in H93, VFJM2, and Branduardi–Raymont et al. (1994).

We conclude that the XHS 47.5/22 presents a normal $\log N - \log S$ relation. It is consistent with previous work in the same flux range. The sample of sources with $\rm ML_{exi} \geq 10$

and $f_x > 3.4 \cdot 10^{-14}$ ergs cm^{-2} s^{-1} is complete to the same level as in H93 or VFJM2.

4. Completeness of the AGN samples

4.1. X–ray selected sample

The completeness limit for the X–ray catalogue as a whole is not identical to the completeness limit of the X–ray selected quasar sample. That limit is determined by finite optical telescope time rather than X–ray flux. A fraction of 93% of the objects with fluxes above $2 \cdot 10^{-13}$ ergs cm^{-2} s^{-1} (i.e. 43 of 46) could be identified, dropping to 84% of X–ray sources brighter than $1.5 \cdot 10^{-13}$ ergs cm^{-2} s^{-1}. The value $f_x = 2 \cdot 10^{-13}$ ergs cm^{-2} s^{-1} is therefore taken as a value below which the X–ray sample becomes significantly incomplete.

4.2. Optically selected sample

A limit of $m_b \simeq 17\overset{m}{.}5$ is given in Hagen et al. (1995) which is, however, the completeness of the scans rather than of the quasars found in the HQS, and averaged over the entire survey. The plates in HS 47.5/22 reach deeper but only an estimated value of $m_b \lesssim 18\overset{m}{.}5$ was given by the HQS group (Engels, priv. comm.). Four X–ray selected AGN with $m_b < 18\overset{m}{.}6$ were found during the follow–up observations for the present project (Paper I). All four match the HQS selection criteria (Engels et al. 1998) and are thus added to the optically selected sample. The three optical counterparts of RX J1001.5+4659 have $m_b \leq 18\overset{m}{.}04$, but their images are clearly extended. Therefore, they do not fulfill the HQS selection criteria and are rejected.

We created the number–magnitude diagram for the optical sample and compared it with other samples of known completeness. Two such samples can be found in Boyle et al. (1988, 'AAT sample') and Hewett et al. (1995). The former consists of 420 faint ($m_b \gtrsim 17^m$), UV excess selected quasars observed at high galactic latitudes. The authors claim a remaining incompleteness of not more than $\sim 10\%$ (Boyle et al., 1988). The second sample is the LBQS sample, consisting of 1055 quasars with $m_b \gtrsim 16^m$. Several search techniques are used, and Hewett et al. (1995) estimate a completeness of $\sim 90\%$, similar to the AAT sample. The third is from Hartwick & Schade (1990) who combined all surveys then available, obtaining more than 1200 quasars with $12\overset{m}{.}5 < m_B < 23^m$. For this work, only the case of $z \leq 2.2$ is relevant because the optical sample contains only two quasars with higher z.

Fig. 3 shows the number–magnitude relations for these 4 samples. In HS 47.5/22, the same area being accessible for all magnitudes, the error σ can simply be computed as $\sigma = \sqrt{N}\,/\,A$, where N is the number of objects in a given magnitude bin. All surface densities and corresponding errors are calculated in $0\overset{m}{.}5$ bins and multiplied by a factor 2 to express them as numbers per unit magnitude. The first binning ($*$ in the plot) is adjusted to Boyle et al. (1988, their Fig. 2).

At magnitudes $m_b < 18\overset{m}{.}2$, the optical sample agrees with the LBQS within the errors. Incompleteness is evident at $m_b > 18\overset{m}{.}6$. This incompleteness remains even if the optically fainter

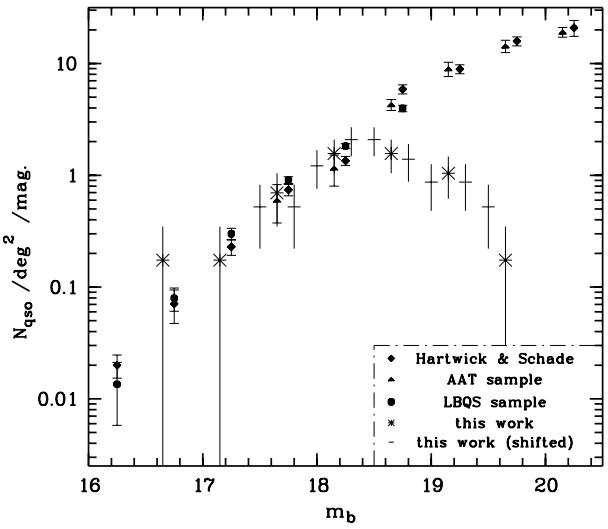

Fig. 3. Number–magnitude relation for the optical sample. The shifted bins are displaced by $0\overset{m}{.}15$ in either direction of the original bin.

X–ray identifications are taken into account. As a check the optical sample is rebinned with the bin centres shifted $0\overset{m}{.}15$ in either direction (– in the plot). As can be seen, the bin at $18\overset{m}{.}3$ is still in good agreement with literature values. So also might be the one centred at $18\overset{m}{.}5$, but less well, and any further shifting of the bins towards fainter magnitudes shows that incompleteness sets in immediately beyond. A conservative completeness limit will therefore be $B_{lim} = 18\overset{m}{.}3$, whereas $B_{lim} = 18\overset{m}{.}5$ is an optimistic one.

5. Luminosity functions

The optical luminosity function, its status and problems has recently been reviewed by Wisotzki (1998) who considered quite a number of AGN. Our completeness limit leaves too small a number of objects to improve on it.

We have, however, compared our X–ray luminosity function (XLF) with that derived by Boyle et al. (1993, henceforth BGSSG93). The complete X–ray sample contains 26 AGN with $0.1 < z < 1.9$. Luminosities are computed with a power law index $\alpha_E = 1$ and $H_0 = 50 \frac{km}{s\,Mpc}$, $q_0 = 0.5$. A conversion factor 0.8 was applied to shift the values to the *Einstein* band (0.3 – 3.5 keV) to facilitate comparison with literature values (e.g. BGSSG93; Jones et al. 1997). The differential XLF, $\Phi\,(L, z)$, was calculated following BGSSG93 for their first ($0 \leq z < 0.4$) and second ($0.4 \leq z < 1$) redshift bins. These contain 10 and 15 AGN respectively. The luminosities in the first redshift bin includes $2 \cdot 10^{43}$ ergs s$^{-1} \lesssim L_x^E \lesssim 4 \cdot 10^{44}$ ergs s^{-1}. The AGN are put into two luminosity bins of equal width $\Delta \log L_x^E = 0.65$, and $\Phi(L, z)$ is computed for each bin,

$$\Phi(L, z) = \left(\Sigma V_a^{-1}\right) \left(\Delta\, L_x^E\right)^{-1}.$$

ΔL_x^E is the *linear* width of the luminosity bin in units of 10^{44} ergs s^{-1}. The second redshift bin contains luminosities between $2 \cdot 10^{44}$ ergs s^{-1} and $3 \cdot 10^{45}$ ergs s^{-1}. Here the original binning of BGSSG93 can be used, with the only difference

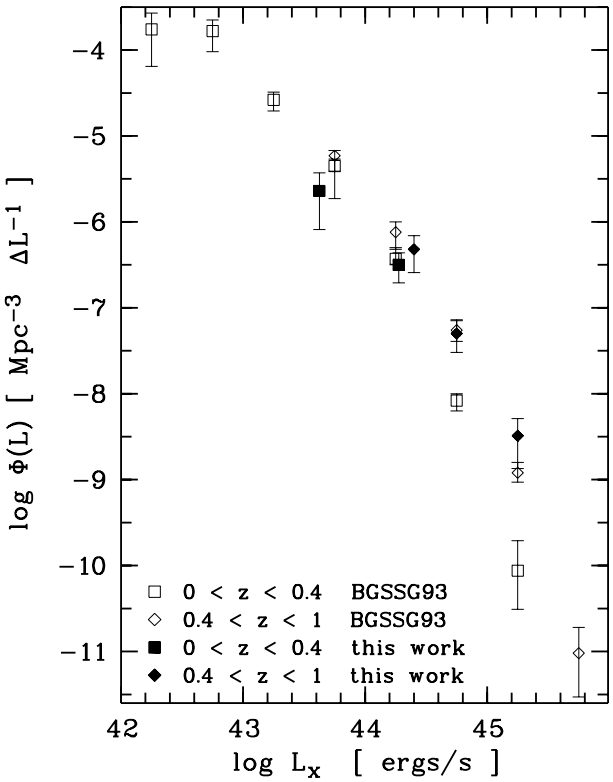

Fig. 4. The differential XLF estimated for two redshift bins. Filled symbols mark values obtained from this work, the open symbols being taken from BGSSG93 (their Fig. 4b).

Table 1. X–ray luminosity function $\Phi(L)$

	$\log L_{\rm x}^{\rm E}$	$\Phi(L)$ $[10^{-8}\,{\rm Mpc}^{-3}(\Delta\,{\rm L})^{-1}]$	σ_Φ
I)	43.63	227	146
	44.28	31.6	21.2
II)	44.40	47.9	21.9
	44.75	5.01	2.01
	45.25	0.322	0.186

that the lowest bin starts at $\log {\rm L}_{\rm x}^{\rm E} = 44.3$. The lower and upper boundaries for the volume integral are set at 0.4 and the minimum of $z_{\rm up} = 1$ and $z_{\rm max}$. Table 1 contains $\Phi({\rm L})$ for the two redshift bins, and the values are compared with BGSSG93 in Fig. 4. The results agree within the errors. A suspicion was raised in Paper I and by Molthagen et al. (1994) that the HS 47.5/22 field might show a non–random AGN distribution. The above results do not give supporting evidence for such a claim.

6. Notes on individual objects

6.1. RX J0952.5+4603 and RX J0953.9+4617

Spectra of the AGN candidates RX J0952.5+4603 and RX J0953.9+4617 were obtained on March 6, 1997 with the 3.5 m telescope at Calar Alto. The telescope was equipped with the focal reducer MOSCA (f/2.7), and both spectra were taken

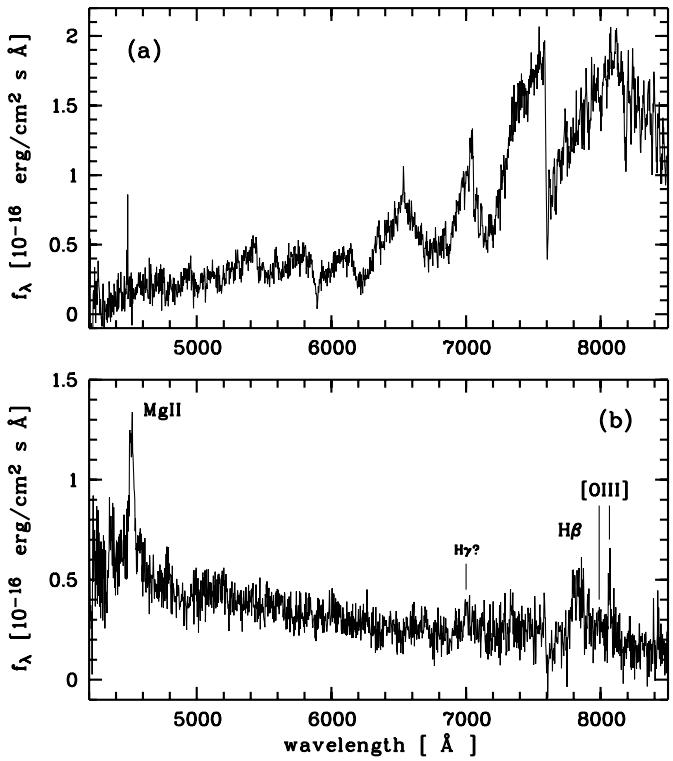

Fig. 5. Spectra of (a) RX J0952.5+4603 and (b) RX J0953.9+4617; f_λ is plotted against observed wavelength.

Table 2. Optical and X–ray parameters of RX J0953.9+4617.

	RX J0953.9+4617
R.A. (J2000.0)	$9^h\ 53^m\ 59\overset{\rm s}{.}2$
DEC. (J2000.0)	$46^\circ\ 17'\ 18''$
z	0.612 ± 0.001
m_b	$19\overset{\rm m}{.}8 \pm 0\overset{\rm m}{.}5$
M_b^a	-23.4
f_x	$(2.18 \pm 0.43) \cdot 10^{-13}\ {\rm ergs\,cm^{-2}\,s^{-1}}$
$L_x^{\rm a}$	$4.4 \cdot 10^{44}\ {\rm ergs\,s^{-1}}$
$N_{H,gal}{}^{\rm b}$	$1.29 \cdot 10^{20}\,{\rm cm^{-2}}$

[a]: $H_0 = 50 \frac{\rm km}{\rm s\,Mpc}$, $q_0 = 0.5$
[b]: error $\simeq 20\%$

with a resolution of 12 Å ($4300 - 8200$ Å). The exposure times for both objects are 400 s. Fig. 5 shows the spectra. The former clearly is a late type star, and therefore of no interest for the present paper. RX J0953.9+4617, on the other hand, shows a typical AGN spectrum with four emission lines which can be identified as Mg II, H β, [O III] 4959 and [O III] 5007. These lines lead to a redshift $z = 0.612 \pm 0.001$. Its observed and calculated properties are summarized in Table 2.

6.2. RX J1001.5+4659

The source RX J1001.5+4659 is located in the central parts of two pointings taken within one year, and visible in both, with a hard band count rate of $2.5 \cdot 10^{-3}\ {\rm cts\,s^{-1}}$. In the merged data,

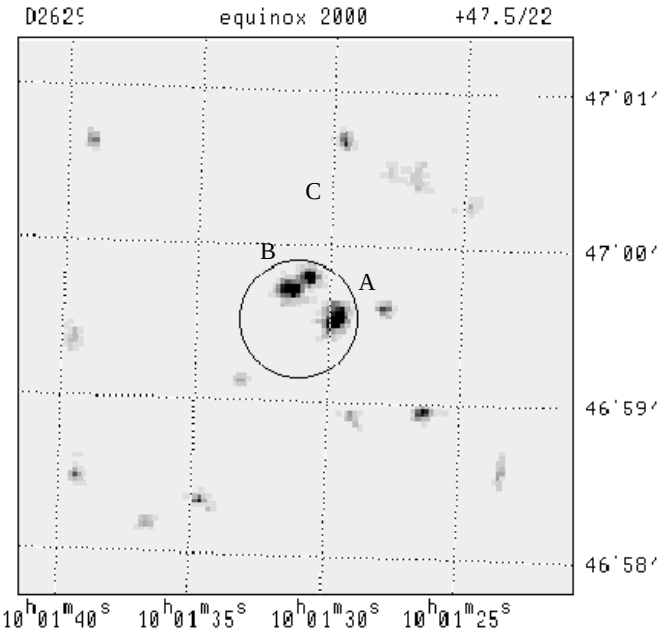

Fig. 6. RX J1001.5+4659 with its three optical counterparts. The circle marks the X–ray position error. The coordinates are J2000.0.

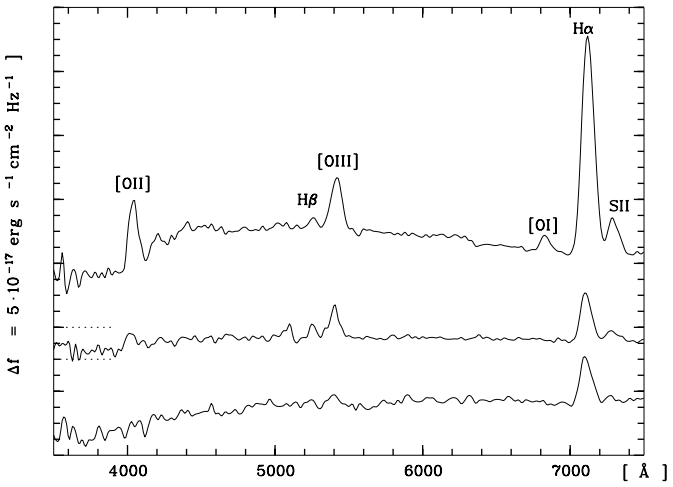

Fig. 7. Spectra of objects A, B and C (top to bottom). The offsets for A and B are $4 \cdot 10^{-16}$ ergs cm^{-2} s^{-1} and $3 \cdot 10^{-16}$ ergs cm^{-2} s^{-1} respectively (dashed lines).

RX J1001.5+4659 is clearly detected with a count rate corresponding to $f_x \simeq 3 \cdot 10^{-14}$ erg cm^{-2} s^{-1} in the total ROSAT band. The error circle of RX J1001.5+4659 contains three optical counterparts of similar apparent magnitude (Fig. 6) and small but definite extension. All three, separated by $9''$ to $21''$, are possible identifications. They were observed in March 1994 (Paper I) and found at a common redshift of $z = 0.08$ (Fig. 7). Objects A and B show indications of Seyfert– or starburst activity (strong S II– and forbidden O–lines in A, blue continuum in B), whereas object C looks more like a normal galaxy. It coincides both in position and redshift with the infrared source IRAS 09583+4714 of Strauss et al. (1992). The infrared emission hints at a high star formation rate somewhere within this group.

The position resolution of the PSPC, especially at such a low count rate level,is insufficient to decide which of the possibilities is correct, namely one point source due to one of the galaxies, two or three point sources due to two or three galaxies, or, most intriguing, one (extended) source connected with the group of galaxies. Although the hardness of the source would not favour the intragroup hot gas interpretation, the possibility should be investigated.

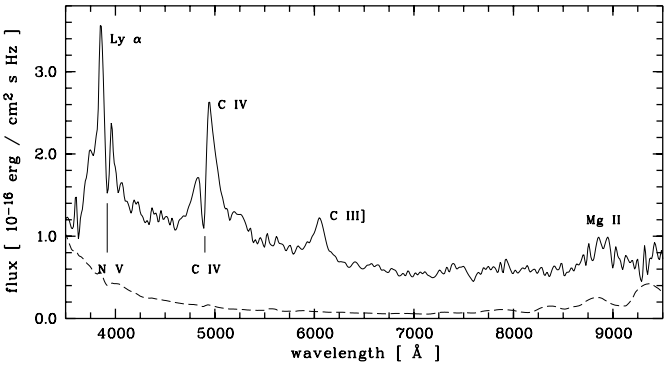

Fig. 8. Optical spectrum of RX J0957.1+4815. The dashed line indicates the noise spectrum.

Table 3. X–ray and optical parameters of RX J0957.1+4815

	X–ray	optical
R.A.	$9^h\,57^m\,8\overset{s}{.}8$	$9^h\,57^m\,9\overset{s}{.}0$
DEC.	$48^\circ\,15'43''$	$48^\circ\,15'44''$
$\sigma_{\rm pos}$	$25''$	$\leq 2''$
$\rm cr_h$	$(2.6 \pm 0.6) \cdot 10^{-3}$ cts s^{-1}	
bright–ness	$(1.4 \pm 0.3) \cdot 10^{-14}$ ergs cm^{-2} s^{-1}	$19\overset{\rm m}{.}14 \pm 0\overset{\rm m}{.}15$
$\rm N_{H,gal}$	$1.02 \cdot 10^{20}$ cm^{-2}	
$\rm z_{em}$	2.170 ± 0.005	
$\rm z_{abs}$	2.157 ± 0.004	

6.3. RX J0957.1+4815

Source #399 is significantly detected in the hard (0.5 – 2.0 keV) and h2 (0.9 – 2.0 keV) bands only, with likelihoods of 15.7 and 23.4 respectively. The 47 ± 11 photons with a net exposure time of $t = 18270$ s result in a count rate $\rm cr_h = (2.6 \pm 0.6) \cdot 10^{-3}$ cts s^{-1}. The source is too faint to allow any spectral fit, so that the hard band flux is computed with the assumption of a power law with $\alpha_E = 1$ (mean value for $z \geq 2$ QSOs in Molthagen 1996) and galactic absorption, yielding an $f_{x,h} = (1.4 \pm 0.3) \cdot 10^{-14}$ ergs cm^{-2} s^{-1}. The X–ray parameters of RX J0957.1+4815 are summarized in Table 3. The spectrum and B image were observed in March 1994 and the former is shown in Fig. 8. No further object appeared above a limiting magnitude of $m_b \simeq 22\overset{\rm m}{.}5$ inside the X–ray error circle ($25''$ radius) so that the identification is unambiguous.

Emission lines of Ly α, C IV1549and C III]1909 can easily be recognized. The former two lines are affected by absorption lines so that only the latter can be used to determine the emission redshift which is found to be $z_{em} = 2.170 \pm 0.005$. The broad bump around 8850 Å can be identified with MgII 2798, but the noise is comparatively high, and the red wing overlaps with an instrumental artefact. The line centre is therefore not well–determined and unsuitable for redshift determination. The two absorption lines are found at 3915 Å and 4892 Å respectively. If they are identified with N V1240 and C IV1549, they give a common absorption redshift of $z_{abs} = 2.157 \pm 0.004$. There are two possible interpretations of the source properties either as a Broad Absorption Line (BAL) QSO or as a QSO with a so–called associated absorption line system.

BAL QSOs are usually X–ray quiet, i.e. with large X–ray to optical indices α_{OX} (Green et al. 1995) and very few have been detected at X–ray frequencies (Green et al. 1995; Green & Mathur 1996). Here $S_{2\,keV}$ is derived from $f_{x,h}$ above. The apparent magnitude is $m_b = 19\overset{m}{.}14 \pm 0\overset{m}{.}15$. Evaluating the flux according to Weedman (1988, his Eq. 3.15a), which is then transformed to 2500 Å and K–corrected using a power law spectrum with $\alpha_{opt} = 0.7$, we obtain $S_{2500Å} = 4.6 \cdot 10^{-28}\ \mathrm{ergs\,cm^{-2}\,s^{-1}\,Hz^{-1}}$ and $S_{2\,keV} = 2.1 \cdot 10^{-32}\ \mathrm{ergs\,cm^{-2}\,s^{-1}\,Hz^{-1}}$. This results in $\alpha_{OX} = 1.7$, consistent with the limit of $\alpha_{OX} \geq 1.6$ required by Green et al. (1995). Its non-detection in the soft band (0.1 – 0.4 keV) and its highest likelihood in the h2 band is consistent with the strong intrinsic absorption (Mathur et al. 1995; Green & Mathur 1996) and is circumstancial evidence in support of the BAL hypothesis. The FWHMs of the two absorption lines (observer's frame) are 50 ± 12 Å $\hat{=} 3800\ \mathrm{km\,s^{-1}}$ (N V) and 49 ± 5 Å $\hat{=} 3000\ \mathrm{km\,s^{-1}}$ (C IV), sufficient to pass the threshold for BAL QSOs given by Weyman et al. (1991). These widths are close to the instrumental resolution but no meaningful deconvolution is possible and the intrinsic line width could be too small to fit the BAL hypothesis. The second criterion of Weyman et al. (1991), a shift to the blue of at least $3000\ \mathrm{km\,s^{-1}}$ with respect to the emission lines, is not met with $v = c\,[(1 + z_{em})^2 - (1 + z_{abs})^2] / [(1 + z_{em})^2 + (1 + z_{abs})^2] = 1233\ \mathrm{km\,s^{-1}}$ only.

Another possible explanation is an associated absorption system. Such systems have $z_{abs} \simeq z_{em}$, within $\pm 5000\ \mathrm{km\,s^{-1}}$ of the emission line redshift (Foltz et al. 1988). This is the case for RX J0957.1+4815, but other circumstances fit less well into the picture. Associated C IV absorption lines are called strong if their rest frame equivalent widths are $REW \geq 1.5$ Å. Foltz et al. (1988) find $REW > 1.5$ Å in 22 out of 88 cases, and only five quasars with $REW > 6$ Å. RX J0957.1+4815 has a measured equivalent width of $REW_{C\,IV} \simeq 8...9$ Å, which would make it very unusual for an associated absorption system.

RX J0957.1+4815 is not detected at radio wavelengths; the $3\,\sigma$ upper limits in 21 cm and 74 cm DRAO data are 2 mJy and 30 mJy respectively (Wendker, priv. comm.). The NVSS (Condon et al. 1998) does not contain a source close enough, thus indicating an upper limit around $1\,\mathrm{mJy}$. Della Ceca et al. (1994) use the radio to optical index α_{ro} to define radio loudness. (Using a range $-3.2 \lesssim \alpha_{ro} \lesssim 2$ (Véron–Cetty & Véron 1996) one would expect $9 < f_{21cm} < 15\,\mathrm{mJy}$ and $15 < f_{74cm} < 25\,\mathrm{mJy}$ in the radio loud case.) We obtain $\alpha_{ro} \leq 0.18$ using the 21 cm upper limits with a weak dependence on the assumed radio spectral index ($\alpha_r < 0.0$). Thus, RX J0957.1+4815 is most probably radio quiet. This supports the BAL hypothesis but at the same time does not contradict the associated absorption explanation. Although associated absorption may be found preferentially in radio loud quasars, it is observed in radio quiet ones as well (Barthel 1991).

With the present data alone, it is impossible to rule out either possibility, but we would like to call RX J0957.1+4815 a BAL candidate. If it turns out to be indeed a BAL QSO, it would be one of the very first X–ray selected BAL QSOs. If the associated system interpretation turns out to be correct it would be comparatively strong, and one of the few found in optically faint, radio quiet quasars.

7. Summary

One motivation at the beginning of this study was that the QSO distribution on the sky showed an apparent inhomogeneity at the margin of statistical significance. Optical identifications increased the number of known quasars from 27 to 71. These were subjected to statistical studies.

After removal of extended objects, stars and stellar candidates the remaining sample is most likely extragalactic. Four more AGN with $m_b < 18\overset{m}{.}6$ were found in this work and added to the HQS sample prior to optical completeness tests. This was done by a comparison of the number–magnitude relation seen here with other surveys of known completeness. A conservative completeness limit is $m_b = 18\overset{m}{.}3$. The $\log N(>S) - \log S$ relation is consistent with literature values (Wisotzki 1998).

At X–rays frequencies, the completeness limit is determined by the identification status. Up to 93% of the sources with $f_x \geq 2 \cdot 10^{-13}\ \mathrm{ergs\,cm^{-2}\,s^{-1}}$ are identified, dropping to 84% at $f_x \geq 1.5 \cdot 10^{-13}\ \mathrm{ergs\,cm^{-2}\,s^{-1}}$; $f_x = 2 \cdot 10^{-13}\ \mathrm{ergs\,cm^{-2}\,s^{-1}}$ is therefore used as a complete sample of 26 AGN.

The X–ray sample is larger than the optical one, and the spread in z is smaller. Ten and fifteen AGN are found in the lower two redshift bins of Boyle et al. (1991). The resulting X–ray luminosity functions agree well with the literature. Three objects with $f_x \geq 2 \cdot 10^{-13}\ \mathrm{ergs\,cm^{-2}\,s^{-1}}$ have no measured redshifts, but unless they are all quasars with redshifts at the upper boundary of the respective redshift bins, they can not lead to significant deviations.

A few objects were presented in detail. New observations of RX J0952.5+4603 and RX J0953.9+4617, two previous AGN candidates with high X–ray fluxes in Paper I, were obtained. The former turned out to be a late type star while the latter is indeed a quasar of redshift $z = 0.612$ and luminosity $L_x = 4.3 \cdot 10^{44}\ \mathrm{ergs\,s^{-1}}$.

One of the newly identified quasars, RX J0957.1+4815, showed deep absorption lines of C IV and N V in its optical spectrum. The resolution of the spectrum is too low to decide

whether RX J0957.1+4815 is indeed a BAL QSO, or rather shows associated absorption. If it were the former, it would be one of the first X–ray selected. If the latter is true, it would be one of the few such systems found in optically faint, radio quiet quasars, and thus still remarkable.

RX J1001.5+4659 is a faint, hard X–ray source with a group of galaxies at a common redshift $z = 0.08$ as possible optical counterpart. Two galaxies show Seyfert or starburst activities, the third seems more normal. It is not clear whether the observed emission is caused by one or more point sources, or by the group as a whole.

Although the number of identified quasars has been nearly tripled there is no supporting evidence in the distribution functions that any significant deviation from previous results occurs in this field. The contrast between the quasar–rich and quasar–poor regions, quite prominent in the beginning, has been substantially weakened by the newly identified objects.

Acknowledgements. I wish to thank N. Bade for his help with the optical observations in 1994 and for taking two more spectra in 1997, S. Köhler for her very useful comments on QSO absorption lines, H. J. Wendker for many useful comments and his help with the paperwork, and J. Hazlehurst for reading the manuscript. My work has been supported by a grant from the BMFT (DARA FKZ 50 OR 9308).

References

Barthel P.D., 1991, ESO Sci.Rep. No 9, p. 79
Boyle B.J., Shanks T., Peterson B.A., 1988, MNRAS 235, 935
Boyle B.J., Jones L.R., Shanks T., et al., 1991, In: Crampton D. (ed.) The Space Distribution of Quasars. p. 191
Boyle B.J., Griffiths R.E., Shanks T., Stewart G.C., Georgantopoulos I., 1993, MNRAS 260, 49 (BGSSG93)
Branduardi-Raymont G., Mason K.O., Warwick R.S., et al., 1994, MNRAS 270, 947
Condon J.J., Cotton W.D., Greisen E.M., et al., 1998, AJ 115, 1693
Della Ceca R., Zamorani G., Maccacaro T., et al., 1994, ApJ 430, 533
Engels D., Hagen H.-J., Cordis L., et al., 1998, A&AS 128, 507
Foltz C.B., Chaffee F.H., Weyman R.J., Anderson S.F., 1988, In: Blades J.C., Turnshek D.A., Norman C.A. (eds.) QSO Absorption Lines: Probing the Universe, p. 54
Gioia I.M., Maccacaro T., Schild R., et al., 1990, ApJS 72, 567
Green P.J., Mathur S., 1996, ApJ 462, 637
Green P.J., Schartel N., Anderson S.F., et al., 1995, ApJ 450, 51
Hagen H.–J., Groote D., Engels D., Reimers D., 1995, A&AS 111, 195
Hartwick F.D.A., Schade D., 1990, ARA&A 28, 437
Hasinger G., Burg R., Giacconi R., et al., 1993, A&A 275, 1 (H93)
Hewett P.C., Foltz C.B., Chaffee F.H., 1995, AJ 109, 1498
Jones L.R., McHardy I.M., Merrifield M.R., et al., 1997, MNRAS 285, 547
Mathur S., Elvis M., Singh K.P., 1995, ApJ 455, L9
Molthagen K., 1996, Ph.D. thesis, Hamburg University
Molthagen K., Wendker H.J., Briel U.G., 1994, IAU Symp. 159, 517
Molthagen K., Wendker H.J., Briel U.G., 1997, A&AS 126, 509 (Paper I)
Pfeffermann E., Briel U.G., Hippmann H., et al., 1986, Proc. SPIE 733, 519
Strauss M.A., Huchra J.P., Bavis M., et al., 1992, ApJS 83, 29
Trümper J., 1983, Adv. Space Res. 2, No. 4, 241
Véron-Cetty M.-P., Véron P., 1996, ESO Sci. Rep. No 17
Vikhlinin A., Forman W., Jones C., Murray S., 1995a, ApJ 451, 542 (VFJM1)
Vikhlinin A., Forman W., Jones C., Murray S., 1995b, ApJ 451, 553 (VFJM2)
Weedman D., 1988, Quasar Astronomy. Cambridge Astrophysics Series, 2nd edition
Weymann R.J., Morris S.L., Foltz C.B., Hewett P.C., 1991, ApJ 373, 23
Wisotzki L., 1998, Astron. Nachr. 319, 257